Biochimica et Biophysica Acta, 732 (1983) 607–619
Elsevier

BBA 71780

PROPERTIES OF THE Mg^{2+}-INDUCED LOW-AFFINITY NUCLEOTIDE BINDING SITE OF ($Na^+ + K^+$)-ACTIVATED ATPase *

F.M.A.H. SCHUURMANS STEKHOVEN, H.G.P. SWARTS, J.J.H.H.M. DE PONT and S.L. BONTING

Department of Biochemistry, University of Nijmegen, Geert Grooteplein Noord 21, P.O. Box 9101, 6500 HB Nijmegen (The Netherlands)

(Received December 6th, 1982)
(Revised manuscript received May 5th, 1983)

Key words: ($Na^+ + K^+$)-ATPase; Nucleotide binding site; Ouabain; Nucleotide specificity; Kinetics; Low-afffinity site; (Rabbit kidney)

(1) The Mg^{2+}-induced low-affinity nucleotide binding by ($Na^+ + K^+$)-ATPase has been further investigated. Both heat treatment (50–65°C) and treatment with *N*-ethylmaleimide reduce the binding capacity irreversibly without altering the K_d value. The rate constant of inactivation is about one-third of that for the high-affinity site and for the ($Na^+ + K^+$)-ATPase activity. (2) Thermodynamic parameters ($\Delta H°$ and $\Delta S°$) for the apparent affinity in the ATPase reaction (K_m ATP) and for the true affinity in the binding of Ado*PP*[NH]*P* (K_d and K_i) differ greatly in sign and magnitude, indicating that one or more reaction steps following binding significantly contribute to the K_m value, which thus is smaller than the K_d value. (3) Ouabain does not affect the capacity of low-affinity nucleotide binding, but only increases the K_d value to an extent depending on the nucleotide used. GTP and CTP appear to be most sensitive, ATP and ADP intermediately sensitive and Ado*PP*[NH]*P* and AMP least sensitive to ouabain. Ouabain reduces the high-affinity nucleotide binding capacity without affecting the K_d value. (4) The nucleotide specificity of the low-affinity binding site is the same for binding (competition with Ado*PP*[NH]*P*) and for the ATPase activity (competition with ATP): Ado*PP*[NH]*P* > ATP > ADP > AMP. (5) The low-affinity nucleotide binding capacity is preserved in the ouabain-stabilized phosphorylated state, and the K_d value is not increased more than by ouabain alone. (6) It is inferred that the low-affinity site is located on the enzyme, more specifically its α-subunit, and not on the surrounding phospholipids. It is situated outside the phosphorylation centre. The possible functional role of the low-affinity binding is discussed.

Introduction

Recently, we have reported evidence for the occurrence of low-affinity nucleotide binding to the ($Na^+ + K^+$)-ATPase complex, in addition to the high-affinity nucleotide binding involved in its phosphorylation [1]. This was accomplished by binding studies with the non-phosphorylating ATP analogue adenylyl-imidodiphosphate (Ado*PP*[NH]*P*). The K_d value for this compound at millimolar Mg^{2+} is 0.2 mM (compared to 0.04 mM for the high-affinity site), binding requires millimolar Mg^{2+} and the binding capacity is one per $\alpha\beta$-dimer.

Further studies of the low-affinity nucleotide binding have been directed to: (1) establishing beyond doubt that binding takes place on the ($Na^+ + K^+$)-ATPase molecule; (2) testing the specificity of the binding site; (3) obtaining more insight in the functional role of low-affinity substrate binding.

* This is the 50th article in the series, Studies on ($Na^+ + K^+$)-activated ATPase. The previous article is Ref. 14.

Materials and Methods

Enzyme preparation and binding assays

Preparation of highly purified $(Na^+ + K^+)$-ATPase from rabbit kidney outer medulla, performance of the nucleotide (adenylylimidodiphosphate ≡ Ado*PP*[NH]*P*) binding assay via a filtration method (with correction for nonspecific retention from the [^{3}H]Ado*PP*[NH]*P*/[^{14}C]sucrose ratio), and determination of K_d values and binding capacities from Scatchard plots have been previously described [1]. The standard binding medium contains 50 mM imidazole-HCl + 5 mM $MgCl_2$ (pH 7.0; ionic strength, 40 mM), 1 mg protein/ml and a range of [^{3}H]Ado*PP*[NH]*P* concentrations, usually 2–300 μM. Blanks containing 10 mM non-radioactive Ado*PP*[NH]*P* are subtracted.

Enzyme assays

The $(Na^+ + K^+)$-ATPase activity has been assayed by the radioactivity method of Schoot et al. [2], which permits the use of micromolar ATP concentrations and restricts the determination of liberated phosphate to that from ATP in the competition experiments described below. [γ-^{32}P]ATP (Amersham, International, U.K.) is mixed with non-radioactive ATP to a specific radioactivity of 0.1–2500 Ci/mol. The K_m value at low (0.2–4 μM) and high (10–5000 μM) ATP concentrations are deduced from Scatchard plots with mutual correction as in the nucleotide binding assay, assuming both activities to represent different steps in the reaction pathway, e.g., spontaneous versus K^+-stimulated hydrolysis. Mg^{2+} at a concentration of 0.1 mM in excess of the ATP concentration provides optimal $(Na^+ + K^+)$-ATPase activity. The controls containing 0.1 mM ouabain and no K^+ have 5 mM Mg^{2+} present throughout. The enzyme concentration (μg protein/ml) in the assay medium is varied in order to obtain measurable activities (%ATP hydrolysis ranging between 2 and 39), as follows: 0.066 at 0.2–1.0 μM ATP, 0.17 at 1.5–2 μM ATP, 0.33 at 50–300 μM ATP, 0.83 at 600–5000 μM ATP, all at 37°C, while at 30, 20 and 11°C the enzyme concentrations are increased by factors 2, 5 and 25, respectively. In the Scatchard plots the mean of the initial and the 10-min ATP concentrations is taken.

Nucleotide competition experiments

At high (0.2–2 mM) ATP concentrations, 5 mM Mg^{2+} is used to reach a suitable compromise between optimal ATPase activity (0.5–1.3 μg/ml enzyme protein at 30–37°C, 4.3 μg/ml at 20°C and 23 μg/ml at 11°C) and optimal exposure of the low-affinity nucleotide binding sites [1]. Competing nucleotides and their final concentrations are: ADP (0.2–1.2 mM), AMP (4–16 mM), Ado*PP*[NH]*P* (0.1–0.4 mM), GTP (0.2–1 mM), CTP (0.1–0.5 mM) and ITP (5–30 mM). All nucleotides are obtained from Boehringer-Mannheim, GmbH, Biochemica, F.R.G. as the disodium salts (ATP, CTP, GTP and ITP), tetralithium salt (Ado*PP*[NH]*P*) or free acid (ADP, AMP). The tetralithium salt of Ado*PP*[NH]*P* is converted to its imidazole salt as previously described [1]. The other nucleotide solutions are brought to pH 7.4 with imidazole. In the case of disodium-ITP, the NaCl concentration in the reaction medium is reduced by an equivalent amount, thus keeping $[Na^+]$ at 100 mM. AMP and ITP are added as magnesium salts in order to avoid an undesirable side-effect by complexation of excess free Mg^{2+} at the high concentrations required for these nucleotides (see under Results). The reaction is started by simultaneous addition of [γ-^{32}P]ATP and another non-radioactive nucleotide and is stopped after 10 min. The K_i and K_m values are determined from Dixon and Lineweaver-Burk plots.

Unless otherwise specified, the $(Na^+ + K^+)$-ATPase activity is assayed at 37°C and nucleotide binding is determined at room temperature (22°C). Binding is expressed in nmol/mg protein and specific $(Na^+ + K^+)$-ATPase activity in μmol/mg protein per h, where protein has been determined by the method of Lowry et al. after trichloroacetic acid precipitation [3] using bovine serum albumin as standard. In experiments with Ado*PP*[NH]*P*, ouabain and P_i (see below) we have used $(Na^+ + K^+)$-ATPase preparations of high specific activity (1400–2300 μmol/mg protein per h), which yield binding and phosphorylation capacities of 2.8–4.6 nmol/mg. In determinations of the K_m for ATP and K_i values for the other nucleotides we have used enzyme preparations of somewhat lower specific activity (950–1400 μmol/mg protein per h).

Heat inactivation

Heat inactivation is carried out at specified temperatures (50–65°C) in capped tubes, each containing 125 μl ($Na^+ + K^+$)-ATPase preparation (2.5 mg/ml) in 50 mM imidazole-HCl (pH 7.0). At various time intervals, tubes are removed from the heating bath and are placed in ice. High- and low-affinity binding are assayed at 22°C with 1 mg enzyme protein/ml in 50 mM imidazole-HCl (pH 7.0) and 0.25 mM [^{3}H]Ado*PP*[NH]*P* in the presence of either 2 mM EDTA (high-affinity binding only) or 5 mM $MgCl_2$ (high- plus low-affinity binding, Ref. 1).

Heat inactivation of nucleotide binding has been compared with that of ($Na^+ + K^+$)-ATPase activity, using for the latter the non-radioactive assay method of Schoot et al. [2] at an enzyme protein concentration of 2 μg/ml (15 min incubation at 37°C and pH 7.4). The effect of heat inactivation (40 min, 53°C) on the K_d and binding capacity of the high- and low-affinity sites has been determined from Scatchard plots using the standard assay conditions described above in the section on Enzyme preparation and binding assays.

Inactivation by N-ethylmaleimide treatment

Incubation with *N*-ethylmaleimide (5 mM) is carried out at 37°C in 50 mM imidazole-HCl (pH 7.0) in the presence of 2 mM EDTA. At specified time intervals, 35-μl aliquots are removed from the preincubation mixture and mixed with 5 μl 150 mM dithioerythritol to stop the reaction of the enzyme with the maleimide, giving a protein concentration of 2.5 mg/ml. Subsequent binding of Ado*PP*[NH]*P* to the high- and low-affinity sites is assayed as described above, with 5.8 mM Mg^{2+} (5 mM in excess of the EDTA derived from the preincubation medium) or 2 mM EDTA present.

The effect on nucleotide binding is compared with the inactivation of ($Na^+ + K^+$)-ATPase activity as described in the previous section. The effect of *N*-ethylmaleimide treatment (35 min, 37°C) on the K_d and binding capacity of the high- and low-affinity sites has been determined from Scatchard plots of [^{3}H]Ado*PP*[NH]*P* binding again as described in the previous section, but in the presence of 5.8 mM Mg^{2+}.

Ouabain binding and its effect on nucleotide binding

[^{3}H]Ouabain binding is assayed in the same way as [^{3}H]Ado*PP*[NH]*P* binding, i.e., at 22°C and pH 7.0. The filtration procedure is used to correct for nonspecific glycoside retention by means of the [^{3}H]ouabain/[^{14}C]sucrose ratio. [^{3}H]Ouabain (Amersham, International, U.K.) is mixed with non-radioactive ouabain (E. Merck, Darmstadt F.R.G.) to obtain a specific radioactivity of 100–1000 Ci/mol. The enzyme (0.6–1.0 mg/ml) is incubated for specified times with ouabain in the presence of 5 mM Mg^{2+} and 50 mM imidazole-HCl (pH 7.0). In parallel experiments, 50 mM Na^+ + 5 mM ATP or 5 mM P_i is included in the medium. Blanks, obtained by incubation with a 25-fold excess of non-radioactive ouabain, are subtracted. Subsequently added Ado*PP*[NH]*P* is dissolved in enzyme-free preincubation medium in order to minimize spontaneous dissociation of the enzyme-ouabain complex. It is added in a 1 : 10 volume ratio to the preincubation mixture.

The effect of ouabain on high- and low-affinity nucleotide binding has been tested after 30-min preincubation of the enzyme (2.5 mg/ml) with ouabain in the presence of 5 mM Mg^{2+}, followed by addition of [^{3}H]Ado*PP*[NH]*P* dissolved in enzyme-free preincubation medium (final enzyme protein concentration 1 mg/ml and 1–200 μM [^{3}H]Ado*PP*[NH]*P*). Dissociation of ouabain from the enzyme by the action of the nucleotide is minimized by filtering 40-μl aliquots within 30 s after addition of the nucleotide. Blanks containing 10 mM non-radioactive Ado*PP*[NH]*P* are subtracted.

Binding of other nucleotides to the low-affinity site is tested by competition with [^{3}H]Ado*PP*-[NH]*P* after exclusion of the high-affinity binding and phosphorylating site by pretreatment for 30 min with 1 mM ouabain in the presence of 5 mM Mg^{2+}. The nucleotides are first converted to their imidazole salts as previously described [1]. The procedure is essentially the same as described in the previous paragraph, except that [^{3}H]Ado*PP*[NH]*P* and another non-radioactive nucleotide are added simultaneously to the ouabain-pretreated enzyme. Final concentrations in the assays are for ATP 0.4–2.5 mM, ADP 1–5 mM, AMP 3.6–18 mM, CTP 1.5–7.3 mM, GTP

0.5–2.5 mM, ITP, 1.3–6.6 mM and Ado*PP*[NH]*P* 0.06–0.15 mM. The K_d and K_i values are determined from Lineweaver-Burk and Dixon plots.

Phosphorylation by inorganic phosphate

Phosphorylation by $^{32}P_i$ in the absence or presence of ouabain (1 mM) is determined as previously described [4] at a temperature of 22°C and a protein concentration of 1 mg/ml. Ado*PP*[NH]*P* is subsequently added in enzyme-free preincubation medium (see previous section) at a volume ratio of 1 : 10. Removal of nonspecific radioactive contamination [2] proved to be unnecessary for the current lots of carrier-free $^{32}P_i$ (New England Nuclear Chemicals GmbH, Dreieichenhain, F.R. G.).

The effect of phosphorylation on low-affinity nucleotide binding is tested by preincubating the enzyme (2.5 mg/ml) with 1 mM ouabain + 5 mM Mg^{2+} in the absence or presence of P_i (0.25 mM) for 30 min. Then [^{3}H]Ado*PP*[NH]*P*, dissolved in enzyme-free preincubation medium is added, in a volume ratio of 3 : 2 (final Ado*PP*[NH]*P* concentrations 50–240 μM), and 40-μl aliquots are removed and filtered within 30 s. Blanks containing 10 mM non-radioactive Ado*PP*[NH]*P* are subtracted.

Results

Effect of heating and N-ethylmaleimide treatment

The enzyme can be treated for up to 15 min at 50°C without appreciable loss of $(Na^+ + K^+)$-ATPase activity, while half of this activity is lost within 15 min at 53°C. The time-dependence of the effect of treatment at 53°C is shown in Fig. 1. The plots for enzyme activity and high-affinity nucleotide binding nearly coincide, and they suggest a biphasic process. Mg^{2+}-induced low-affinity nucleotide binding, determined as the difference between total binding and high-affinity binding, shows a monophasic decrease with a rate constant of only 40% of that for high-affinity binding in the second phase. Fig. 2 presents the inactivation of Mg^{2+}-induced low-affinity nucelotide binding at 50, 53 and 65°C. Each temperature step is accompanied by a 10-fold increase in the rate constant of inactivation, which at 50°C is 0.0012 min^{-1} for low-affinity binding, 0.0032 min^{-1} for high-affinity binding and 0.0027 min^{-1} for the ATPase activity. Hence, at 50°C the ratio of the rate constants for inactivation of high- and low-affinity binding is nearly equal to that at 53°C, but both plots are now monophasic.

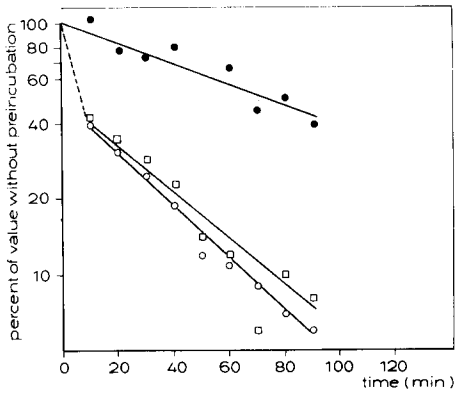

Fig. 1. Heat-inactivation of high-affinity (□) and Mg^{2+}-induced low-affinity (●) Ado*PP*[NH]*P* binding. The enzyme is preincubated at 53°C for the indicated times. The log residual binding relative to that of an untreated sample is plotted vs. time of preincubation. For comparison, heat-inactivation of $(Na^+ + K^+)$-ATPase activity (○) is also plotted. The lines have been calculated by linear regression analysis.

Inactivation by *N*-ethylmaleimide is shown in Fig. 3. The plots for high-affinity nucleotide binding and overall $(Na^+ + K^+)$-ATPase activity nearly coincide, with a rate constant of 0.07 min^{-1}. Inactivation of low-affinity nucleotide binding is nearly 3-times slower, with a rate constant of 0.025

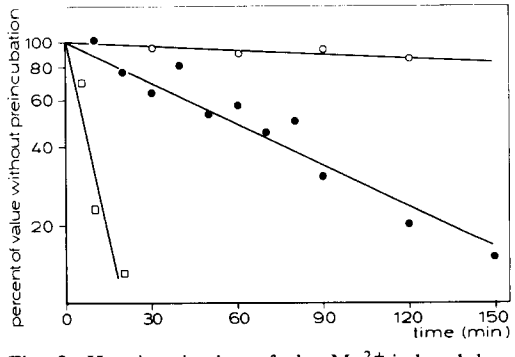

Fig. 2. Heat-inactivation of the Mg^{2+}-induced low-affinity Ado*PP*[NH]*P* binding. The enzyme is preincubated for the indicated times at 50 (○), 53 (●) and 65°C (□). The log residual binding relative to that of an untreated sample is plotted vs. time of preincubation. Lines through the experimental points fitted visually.

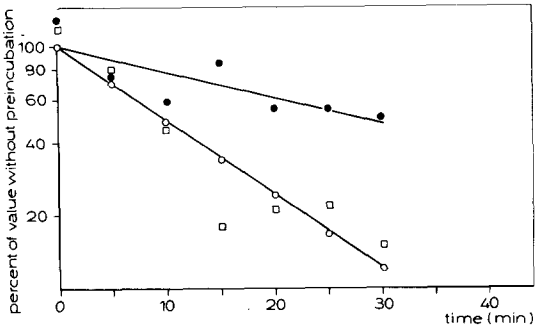

Fig. 3. Inactivation of high-affinity (□) and Mg^{2+}-induced low-affinity (●) Ado*PP*[NH]*P* binding by *N*-ethylmaleimide. The enzyme is preincubated at 37°C with 5 mM *N*-ethylmaleimide for up to 30 min. Log residual binding is plotted vs. time of preincubation. The 100% values have been determined by linear regression analysis from the experimental points. The zero-time values for high- and low-affinity binding, belonging to an untreated sample, happen to be above 100%. For comparison, the inactivation of $(Na^+ + K^+)$-ATPase activity (○) by *N*-ethylmaleimide is also plotted.

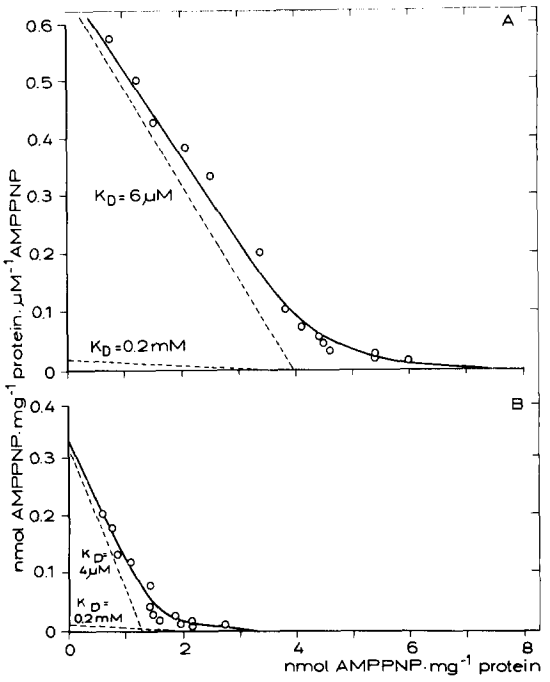

Fig. 4. Effect of heat treatment on high- and low-affinity Ado*PP*[NH]*P* (AMPPNP) binding. A. The native enzyme, without heat treatment, is assayed for nucleotide binding at 22°C in the presence of 5 mM Mg^{2+}. B. The enzyme, after treatment for 40 min at 53°C, is assayed for nucleotide binding in the same way. Each of the curved Scatchard plots has been resolved into two linear plots (dashed lines) by 3-fold mutual correction [1], providing the indicated K_d values and binding capacities.

min^{-1}. In the absence of *N*-ethylmaleimide, the enzyme is stable at the temperature of preincubation (37°C).

The data show that inactivation of low-affinity binding by heating or *N*-ethylmaleimide treatment does not determine the rate of inactivation of the $(Na^+ + K^+)$-ATPase activity. A parallel decrease in high-affinity nucleotide binding capacity and $(Na^+ + K^+)$-ATPase activity following these treatments has previously been demonstrated for an ox-brain preparation [5]. Some of the plots may represent smooth curves rather than straight lines, e.g., heat inactivation of high-affinity binding and ATPase activity (Fig. 1) and inactivation of low-affinity binding by *N*-ethylmaleimide (Fig. 3). Since our primary interest is in the effect of heating or *N*-ethylmaleimide treatment on the nucleotide binding capacities, we have not made a detailed investigation of the kinetics of inactivation.

Inactivation of high- and low-affinity nucleotide binding by heating or *N*-ethylmaleimide treatment is reflected in a reduction of the nucleotide binding capacities without significant reduction of the binding affinities. This is revealed by comparing Scatchard plots (Fig. 4) of nucleotide binding in the presence of 5 mM Mg^{2+}, with and without pretreatment with heat or *N*-ethylmaleimide (Table I). The loss of binding capacity compares fairly well with the reduction of binding at a single nucleotide concentration (Figs. 1–3) after equally long pretreatment as in Table I.

Maximal binding capacity, $E\text{-}A_{max}$, for the low-affinity binding of the controls (Table I) is lower than the maximal binding capacity at the high-affinity sites. This is possibly due to 5 mM Mg^{2+} being submaximal for these preparations. With a K_d value of 0.8 mM [1] for the induction by Mg^{2+} of the low-affinity sites, a ratio of actual binding over maximal binding capacity $E\text{-}A/E\text{-}A_{max}$ of $5/5.8 = 0.86$ is calculated. Since $E\text{-}A_{max}$ for high- and low-affinity binding should be equal [1], the calculated low-affinity binding at 5 mM Mg^{2+} should be 3.3 and 3.5 nmol/mg protein, which values are not significantly different from the control values (3.1 and 3.1) shown in Table I. There is, however, some variability in the Mg^{2+} K_d

TABLE I

EFFECTS OF HEATING AND *N*-ETHYLMALEIMIDE TREATMENT ON HIGH- AND LOW-AFFINITY Ado*PP*[NH]*P* BINDING

Enzyme is heated for 40 min at 53°C or treated with *N*-ethylmaleimide (5 mM) for 35 min at 37°C. Maximal binding capacities ($E\text{-}A_{max}$) and K_d values have been determined for controls and treated samples from Sctachard plots as shown in Fig. 4. Data are averages from two experiments with two different enzyme preparations. S.E. has been calculated as 0.63 × range [6]. Values in parentheses indicate residual binding capacity as percent of the control value.

	High-affinity binding		Low-affinity binding	
	$E\text{-}A_{max}$ (nmol/mg protein)	K_d (mM)	$E\text{-}A_{max}$ (nmol/mg protein)	K_d (mM)
Control	3.8 ± 0.3	0.005 ± 0.002	3.1 ± 0.4	0.3 ± 0.1
After heating	1.33 ± 0.04 (35)	0.003 ± 0.001	2.0 ± 0.1 (65)	0.3 ± 0.1
Control	4.1 ± 0.2	0.0037 ± 0.0004	3.1 ± 0.3	0.18 ± 0.03
After *N*-ethylmaleimide treatment	1.0 ± 0.2 (24)	0.0040 ± 0.0001	2.1 ± 0.1 (68)	0.22 ± 0.03

values, as noticed before [1]. This probably explains why, in Table III, for two other preparations the binding capacity is already maximal at 5 mM Mg^{2+}: presumably these preparations have a somewhat lower Mg^{2+} K_d.

Effect of temperature (0–37°C) on high- and low-affinity nucleotide binding

Robinson [7] used as a criterion to distinguish between high- and low-affinity nucelotide binding sites the thermodynamic characterization of their K_m values in the overall $(Na^+ + K^+)$-ATPase reaction. High-affinity binding had a much lower temperature coefficient than low-affinity binding and would be driven by an entropy change, whereas low-affinity binding would be driven by an enthalpy change. We confirm these findings in experiments, where the temperature dependence of the K_m values for the ATPase reaction is determined (Fig. 5). From these experiments we have obtained the thermodynamic parameters shown in Table II. These values are in good agreement with those reported by Robinson [7], especially when taking into account that he used rat brain microsomes and we a purified enzyme preparation from rabbit kidney outer medulla. The corresponding V_{max} values in the 11–37°C temperature range are 0.3–6 and 28–940 μmol/mg protein per h, respectively, i.e., V_{max} with the low K_m value is only 0.6–1% of that with the high K_m value. While the K_m for ATP includes not only rate constants of binding and release but also the rate constants of reactions following binding, the K_i value of a competing low-activity substrate represents the dissociation constant of the enzyme-inhibitor complex if the rate constant of the subsequent reaction is small. We have therefore compared the K_d for binding of Ado*PP*[NH]*P* with its K_i value in the $(Na^+ + K^+)$-ATPase activity (Fig. 5).

In assaying the binding of Ado*PP*[NH]*P*, we observe thermodynamic parameters which are quite different from those for the K_m of ATP. Low-affinity binding rather than high-affinity binding has the low-temperature coefficient and both types of binding turn out to be driven by a change in entropy (Table II). The entropy change even provides the largest contribution to the exergonic standard free energy change of low-affinity binding. This indicates that in the ATPase reaction steps subsequent to binding of ATP have a temperature coefficient different from that for binding and contribute appreciably to the ratio of kinetic constants represented by the K_m value.

This is confirmed by the near coincidence of the plots for log K_i activity vs. $1/T$ and for log K_d binding vs. $1/T$ (Fig. 5). Although these plots have been obtained with two different enzyme preparations, the K_i activity (0.28 mM at 37°C) is near the

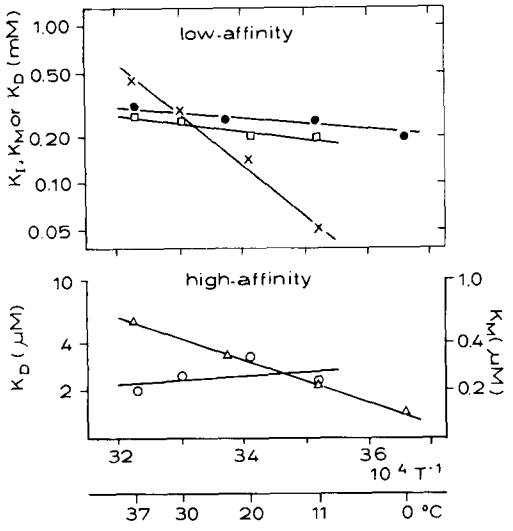

Fig. 5. Semilogarithmic plot of K_m, K_i or K_d versus $1/T$. Meaning of symbols: ● and △, K_d for Ado*PP*[NH]*P* binding in the presence of 5 mM Mg^{2+}; × and ○, K_m for ATP in the $(Na^+ + K^+)$-ATPase reaction with 0.1 mM Mg^{2+} in excess of the ATP concentration; (□) K_i for inhibition of ATPase activity by Ado*PP*[NH]*P* at high (0.2–2 mM) ATP and 5 mM Mg^{2+}. Lines through the experimental points calculated by regression analysis.

average value of 0.33 ± 0.05 mM for five preparations (Table IV) and the K_d binding (0.25 mM at 24°C) is near the average value of 0.20 ± 0.02 mM at 22°C for ten preparations. Moreover, Dixon plots for Ado*PP*[NH]*P* inhibition of ATPase activity at a range of ATP concentrations, covering the low-affinity K_m value (Fig. 5), indicate that competition between the two nucleotides occurs (Fig. 9B), as previously established by Robinson ([7], Fig. 5). In view of their structural analogy [8] we consider it likely that low-affinity binding of Ado*PP*[NH]*P* and ATP takes place at the same site.

Effects of ouabain on high-affinity and low-affinity nucleotide binding

Ouabain, in addition to inhibiting the K^+-stimulated dephosphorylation step in the overall enzyme reaction [9], inhibits high-affinity nucleotide binding [10]. We have determined its effect on low- and high-affinity nucelotide binding. The enzyme preparation is treated with ouabain for 30 min at 22°C in the presence of 5 mM Mg^{2+}, which leads to a steady-state level of ouabain binding

TABLE II

THERMODYNAMIC PARAMETERS OF HIGH- AND LOW-AFFINITY NUCLEOTIDE BINDING

Binding of Ado*PP*[NH]*P* and $(Na^+ + K^+)$-ATPase activity with ATP as substrate are determined under the conditions given in the legend of Fig. 5. $\Delta H°$ is determined from the slopes ($\Delta H°/2.3\ R$) of the semi-logarithmic plots (log K_m, K_i or K_d vs. $1/T$), presented in Fig. 5. $\Delta G°$ is calculated from the formula $\Delta G° = 2.3\ RT \log K_m$, K_i or K_d (K_m, K_i and K_d in mol/l) and $\Delta S°$ from $\Delta G° = \Delta H° - T\Delta S°$.

Site	Process	$\Delta G°$ (37°C) (kcal/mol)	$\Delta H°$ (kcal/mol)	$\Delta S°$ (cal/K per mol)
High-affinity				
	binding [a]	−7.4	−6.0	+4.5
	ATPase [b]	−9.4	+1.3	+34
	ATPase *[b]	−8.5	0	+27
Low-affinity				
	binding [a]	−5.0	−1.7	+10.7
	ATPase [c]	−5.0	−2.2	+9.0
	ATPase [b]	−4.7	−14.1	−30
	ATPase *[b]	−4.7	−10.8	−20

[a] from K_d for Ado*PP* binding.

[b] from K_m for ATP in the ATPase reaction; * data from Robinson [7], included for comparison.

[c] from K_i for Ado*PP*[NH]*P* inhibition in the ATPase reaction.

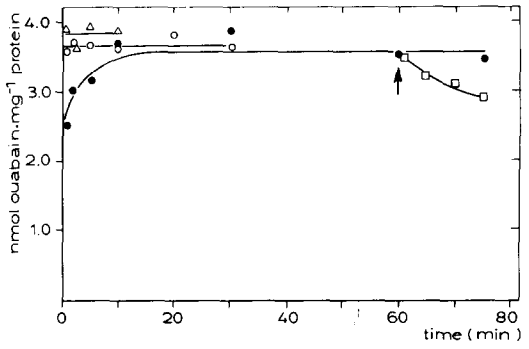

Fig. 6. Effect of Ado*PP*[NH]*P* on ouabain binding. Ouabain binding is measured at 22°C and 200 μM ouabain in the presence of 5 mM Mg^{2+} (●); 5 mM Mg^{2+} + 50 mM Na^+ + 5 mM ATP (△); and 5 mM Mg^{2+} + 5 mM P_i (○). Ado*PP*[NH]*P* (300 μM final concentration) is added after 60 min (arrow) to the medium containing 5 mM Mg^{2+}, and binding (□) is followed for another 15 min in comparison to a nucelotide-free control (●).

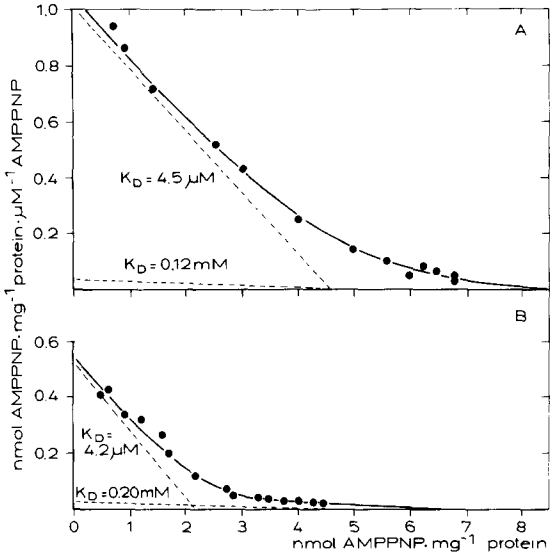

Fig. 7. Effects of ouabain on high- and low-affinity Ado*PP*[NH]*P* (AMPPNP) binding. A Scatchard plot shows Ado*PP*[NH]*P* binding in the presence of 5 mM Mg^{2+} and in the absence of ouabain (A) or the presence of 5 μM ouabain (B). The curved plots have been resolved into two linear plots (dashed lines) by 3-fold mutual correction [1], providing the indicated K_d values and binding capacities.

(Fig. 6). The maximal level obtained is 3.6 nmol/mg protein, which is nearly the same as the levels obtained in the presence of Mg^{2+} + P_i or ATP + Na^+ + Mg^{2+}. Scatchard analysis of ouabain binding in the presence of 5 mM Mg^{2+} and in the absence of Ado*PP*[NH]*P* reveals a K_d value of 1.1 μM. Subsequent addition of Ado*PP*[NH]*P* at the relatively high level of 300 μM slowly drives ouabain from the enzyme (2% in 1 min, Fig. 6). Similar results are obtained at lower levels of ouabain binding at low ouabain concentrations (5 μM). The nucleotide apparently shifts the equilibrium of ouabain binding by increasing its K_d. Yet, the rate of dissociation is sufficiently slow that by quickly filtering samples the original binding levels of ouabain can nearly be maintained. Therefore, in subsequent experiments we have removed and filtered samples within 30 s after addition of the nucleotide.

Fig. 7 shows Scatchard plots for Ado*PP*[NH]*P* binding in the presence of 5 mM Mg^{2+} and in the presence or absence of ouabain (5 μM). Ouabain at this concentration reduces the high-affinity binding capacity by half without affecting the K_d. The low-affinity nucleotide binding capacity is not changed, but the K_d is slightly increased (Table III). The same pattern is observed at higher ouabain concentrations except for greater reduction of the high-affinity binding capacity. The

TABLE III

EFFECTS OF OUABAIN ON HIGH- AND LOW-AFFINITY Ado*PP*[NH]*P* BINDING

Maximal binding capacities (E-A_{max}) and K_d values have been determined from Scatchard plots as shown in Fig. 7. Two experiments have been carried out with two different enzyme preparations. Values in parentheses indicate residual binding capacity as percent of the control value.

	High-affinity binding		Low-affinity binding	
	E-A_{max} (nmol/mg protein)	K_d (mM)	E-A_{max} (nmol/mg protein)	K_d (mM)
Control	4.6	0.0045	4.4	0.12
+ 5 μM ouabain	2.2 (48)	0.0042	4.4 (100)	0.20
Control	3.6	0.005	3.3	0.23
+ 25 μM ouabain	0.8 (22)	0.0042	3.4 (103)	0.28
+ 100 μM ouabain	0.4 (11)	0.006	3.6 (109)	0.25

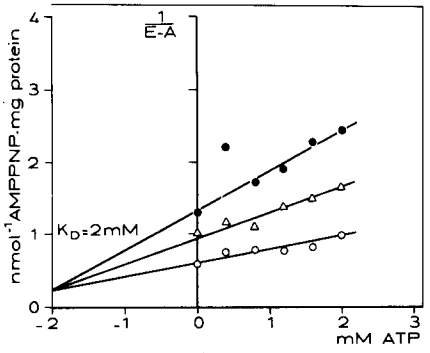

Fig. 8. Low-affinity Ado*PP*[NH]*P* (AMPPNP) binding in the presence of ATP. The reciprocal Ado*PP*[NH]*P* binding (*E-A* in nmol Ado*PP*[NH]*P*/mg protein) is presented in a Dixon plot as a function of the ATP concentration. ATP and Ado*PP*[NH]*P* are added simultaneously to the ouabain-pretreated enzyme yielding the indicated final concentrations (Ado*PP*[NH]*P* (μM); ●, 60; △, 100; ○, 150). The K_i (= K_d) value for ATP is indicated at the intersection in the left-hand quadrant. Lines through the experimental points fitted visually.

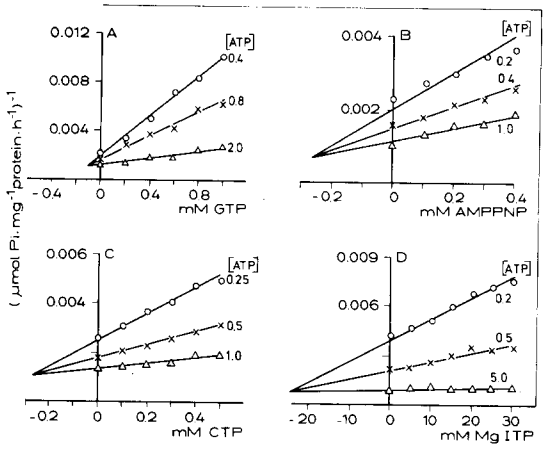

Fig. 9. Competitive inhibition of $(Na^+ + K^+)$-ATPase activity by various nucleotides. The reciprocal specific activities are presented in Dixon plots as a function of the concentration of inhibitory nucleotide at various ATP concentrations (given to the right of each plot in mM). The enzyme activity is assayed in the presence of 5 mM Mg^{2+}, following the simultaneous addition of ATP and GTP (A), Ado*PP*[NH]*P* (AMPPNP, B), CTP (C) or ITP (D). ITP is added together with an equimolar amount of Mg^{2+}. Lines through the experimental points are visually fitted.

increase in the K_d value for low-affinity nucleotide binding has been confirmed in a larger series of experiments with 1 mM ouabain in the presence of 5 mM Mg^{2+}: K_d increases by 65% from 0.20 ± 0.02 mM (n = 10) to 0.33 ± 0.03 mM (n = 13).

Nucleotide specificity of the Mg^{2+}-induced low-affinity binding site

Other nucleotides than Ado*PP*[NH]*P* have been tested for their binding to the Mg^{2+}-induced low-affinity site. In these experiments, 1 mM ouabain is added to prevent binding and phosphorylation via the high-affinity site. The binding is assayed via competition with [^{3}H]Ado*PP*[NH]*P* at three different levels of the latter nucleotide. The results are analyzed by means of a Dixon plot (Fig. 8).

TABLE IV

NUCLEOTIDE SPECIFICITY OF STATICALLY AND KINETICALLY DEFINED LOW-AFFINITY SITES

Comparison of binding specificity to the enzyme-ouabain complex and to the enzyme turning over in the $(Na^+ + K^+)$-ATPase reaction at high ATP level. Presented are K_i, K_d or K_m values of the listed nucleotides as averages with S.E. for n determinations. For n = 2, S.E. = 0.63 × range [6].

Nucleotide	Binding K_i (mM)	n	$(Na^+ + K^+)$-ATPase K_i (mM)	n	Ratio of K_i values
Ado*PP*[NH]*P*	0.33 ± 0.03 [a]	13	0.33 ± 0.05	5	1.0
GTP	1.8 ± 0.3	2	0.12 ± 0.01	3	15
ATP	2.1 ± 0.1	3	0.43 ± 0.04 [b]	7	4.9
ADP	2.5 ± 0.3	3	0.60 ± 0.05	3	4.2
ITP	7.0 ± 1.3	2	23 ± 3.2	2	0.3
CTP	7.9 ± 0.8	2	0.25 ± 0.05	2	32
AMP	8.0 ± 1.3	2	7.5 ± 0.4	2	1.1

[a] K_d value,
[b] K_m value.

The K_i values are presented in Table IV. The highest specificity (K_i 1.8–2.5 mM) is displayed by the purine nucleoside tri- and diphosphates, carrying an amino group in the 6-position (ATP, ADP) or 2-position (GTP). The amino group substituent appears important since ITP, lacking this group, has a much higher K_i value than ATP. CTP contains an amino group in the 6-position, but here the pyrimidine base in the nucleus instead of the purine base apparently leads to a much lower affinity. The β-γ phosphate chain also appears to be important for binding, since AMP has a much lower affinity than ATP and ADP. It is remarkable that the ATP analogue Ado*PP*[NH]*P*, with its β-γ iminophosphate linkage, has the highest affinity ($K_d = 0.33$ mM) of all nucleotides tested for the enzyme-ouabain complex.

The K_i values for low-affinity nucleotide binding in the presence of ouabain are compared with their respective K_m or K_i values in the overall ATPase reaction at high ATP (0.2–2 mM) and Mg^{2+} (5 mM) concentrations (Table IV). Excess Mg^{2+} is added in order to obtain a high level of low-affinity nucleotide binding [1], but it gives about 25% submaximal ($Na^+ + K^+$)-ATPase activity at the concentrations of ATP used. This effect must be on the K_m ATP rather than on V_{max}, since the Dixon plots (Fig. 9) intersect at $1/V_{max}$ of the preparations. The linearity of the plots (slope = $K_m/(V_{max} \cdot K_i[S])$) indicates that competing nucleotides at low concentration do not noticeably affect the K_m ATP by their complexation of Mg^{2+}. The plots have a common intersection, indicating a constant K_i value. However, when the competing nucleotide is added in high concentration (as in the case of ITP with its high K_i value), stimulation of the enzyme activity by complexation of free Mg^{2+} is observed, which is abolished when the nucleotide is added as its magnesium salt (Fig. 9D).

The 0.2–2 mM concentrations of ATP are saturating for the high-affinity site ($K_m = 0.2$ μM, Fig. 5), but are in the range where the partial reaction following low-affinity binding is rate limiting. The K_m for ATP in driving this reaction is 0.43 mM, close to the value (0.5 mM) found by Robinson [7]. The K_i for Ado*PP*[NH]*P* (0.33 mM) agrees with the K_d (0.3 mM at 37°C) for this nucleotide at the low-affinity site in the absence of ouabain (Fig. 5) and also with the K_i value of 0.4 mM reported by Robinson [7]. The K_i and K_m values for binding and ATPase reaction follow the same sequence: Ado*PP*[NH]*P* < ATP < ADP < AMP. In the ATPase reaction, GTP and CTP come before Ado*PP*[NH]*P*, but in binding they follow upon Ado*PP*[NH]*P*. This may be due to the higher ouabain-sensitivity of their binding than for the other nucleotides, as revealed by the high K_i ratio for these nucleotides (Table IV). The binding of Ado*PP*[NH]*P* and AMP appears to be least sensitive to ouabain, considering their K_i ratios of 1.0–1.1 The low ouabain-sensitivity of the low-affinity Ado*PP*[NH]*P* binding has already been documented in Table III. The very low K_i ratio of 0.3 for ITP indicates that binding of this nucleotide may be more sensitive to K^+, present in the ATPase assay medium, than to ouabain, present in the binding medium. The K_i value of 14 mM for ITP in the ($Na^+ + K^+$)-ATPase reaction of an ox-brain cortex preparation [11] is still twice the K_i value found for its binding to the enzyme-ouabain complex in the present experiments.

Binding of AdoPP[NH]P to the phosphoenzyme

In our previous paper [1] we reported that the Mg^{2+}-induced low-affinity nucleotide binding site, in contrast to the high-affinity binding site, is non-phosphorylating. This might imply that the

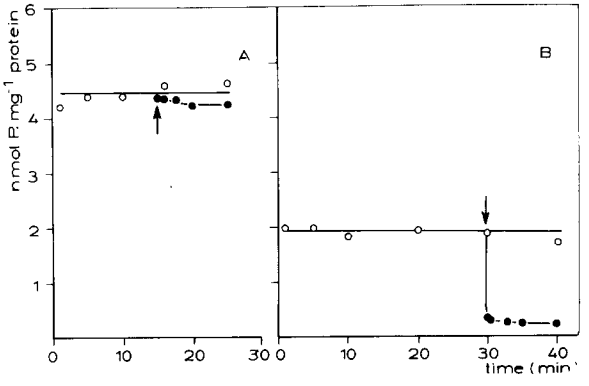

Fig. 10. Effect of Ado*PP*[NH]*P* on the P_i-phosphorylation level. Extent of phosphorylation in the presence of 5 mM Mg^{2+}, 0.25 mM P_i and the presence of 1 mM ouabain (A) or the absence of ouabain (B) is shown. Ado*PP*[NH]*P* is added (final concentration 250 μM) at the indicated time (arrows) and the phosphorylation level in the absence (○) or presence (●) of the nucleotide is followed for another 10 min.

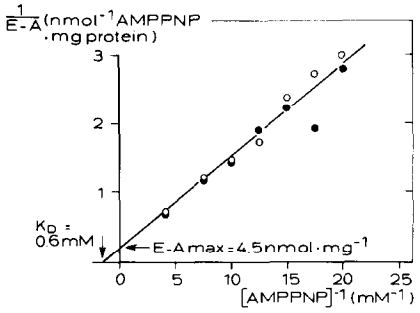

Fig. 11. Low-affinity binding of Ado*PP*[NH]*P* (AMPPNP) to the phosphorylated and nonphosphorylated enzyme. The binding of Ado*PP*[NH]*P* (*E-A*) to the ouabain-pretreated, nonphosphorylated enzyme (●) or the ouabain-pretreated, P_i-phosphorylated (○) enzyme is presented as a function of the Ado*PP*[NH]*P* concentration in a double-reciprocal plot. The concentrations of Mg^{2+}, P_i and ouabain are those given in the legend of Fig. 10. The values of low-affinity nucleotide binding capacity ($E\text{-}A_{max}$) and of K_d for Ado*PP*[NH]*P* are shown. Line through the experimental points visually fitted.

low-affinity site is outside the phosphorylation centre. In order to test this, we have investigated Ado*PP*[NH]*P* binding to the phosphoenzyme. The enzyme is phosphorylated by inorganic phosphate, which leads to the same intermediate as obtained by phosphorylation with ATP [12,13]. It is necessary to stabilize the phosphoenzyme by the presence of ouabain (Fig. 10A), since addition of Ado*PP*[NH]*P* to the phosphoenzyme in the absence of ouabain rapidly drives off the phosphate (Fig. 10B).

Low-affinity binding of Ado*PP*[NH]*P* is presented as a double-reciprocal plot for the phosphorylated and the non-phosphorylated enzyme-ouabain complex in Fig. 11. The low-affinity nucleotide binding capacity is not changed by phosphorylation to the same maximal level as in Fig. 10. Neither does phosphorylation change the nucleotide binding affinity beyond the (increased) K_d value of the enzyme-ouabain complex (Fig. 11).

These experiments prove that Mg^{2+}-induced low-affinity nucleotide binding also occurs on the phosphoenzyme and thus at a site outside the phosphorylation centre.

Discussion

Location of the Mg^{2+}-induced low-affinity site

The purified $(Na^+ + K^+)$-ATPase preparation has a high lipid content, viz., 380 mol phospholipid, 270 mol cholesterol and 100 mol acylglycerols and free fatty acids per mol enzyme protein [14]. Complexation of a lipophilic derivative of ATP, viz., 2′,3′-*O*-(2,4,6-trinitrohexadienylidene) adenosine 5′-triphosphate, to the phospholipid moiety in the presence of Mg^{2+} or Na^+ has been reported [15]. Hence, it is essential to determine whether the Mg^{2+}-induced low-affinity nucleotide binding site is located on the enzyme or on phospholipids.

Heat-inactivation and alkylation of cysteinyl SH groups by *N*-ethylmaleimide should provide means to discriminate between these two possibilities. Heat-inactivation above the optimal temperature is shown by enzymes in the presence as well as the absence of phospholipids. It is rather unlikely that the protein conformational changes involved in heat-inactivation would induce irreversible loss of binding capacity to phospholipids, if the latter were able to form complexes with nucleotides. A similar argument holds for inactivation by *N*-ethylmaleimide, which reacts with protein SH groups under our preincubation conditions but not with the NH_2 groups of phosphatidyl ethanolamine and phosphatidyl serine [16,17]. Hence, we conclude from the decrease in low-affinity nucleotide binding capacity following heating and *N*-ethylmaleimide treatment that this binding takes place on the protein moiety of $(Na^+ + K^+)$-ATPase rather than on the surrounding phospholipids.

N-Ethylmaleimide in the absence of detergent reacts only with the α-subunit of $(Na^+ + K^+)$-ATPase [17]. This would locate the Mg^{2+}-induced low-affinity nucleotide binding site on the α-subunit, which also carries the high-affinity nucleotide binding site [18], the phosphorylation site [19], and (a part of) the ouabain binding site [20]. The site must, however, be located outside the high-affinity binding and phosphorylation centre, since low-affinity binding is additional to high-affinity binding and also occurs on the fully phosphorylated enzyme-ouabain complex. The latter finding also yields a positive answer to one of the questions raised in our previous publication [1], i.e., whether the Mg^{2+}-induced low-affinity binding site is exposed during phosphorylation. Studies of the effect of ATP and P_i on the K^+/K^+ exchange [21] and of ATP on the spontaneous phosphohydroly-

sis of the P_i-phosphorylated enzyme [22] also indicate low-affinity nucleotide binding to the phosphoenzyme.

The conclusion that the low-affinity nucleotide binding site is located on the α-subunit is based on the assumption that *N*-ethylmaleimide modifies an essential SH group in the low-affinity binding centre. The fact that the rate of inactivation is 3-times lower than for the inactivation of an essential SH group in the high-affinity centre is possibly due to a lower accessibility of the low-affinity site to the sulphydryl reagent. The studies by Patzelt-Wenczler and Schoner [23] with a disulphide nucleotide analogue $(6\text{-S-ITP})_2$ support the assumption that the inactivation is the result of a direct effect on the binding centre rather than an allosteric effect, e.g., through α-β subunit interaction. These studies also provide evidence that both binding sites contain an essential SH group, but here the rate of inactivation of the low-affinity binding site is even 20-times lower than that for the high-affinity binding site.

Function of the Mg^{2+}-induced low-affinity nucleotide binding

With the newly acquired knowledge of the properties of Mg^{2+}-induced low-affinity nucleotide binding, we can attempt to discuss the possible role of this binding in the $(Na^+ + K^+)$-ATPase reaction mechanism. Low-affinity binding of Mg^{2+} and ATP must have functional importance, since the rate of $(Na^+ + K^+)$-ATPase at millimolar ATP and Mg^{2+} is more than 100-times as fast as at micromolar ATP, even though the high-affinity binding and phosphorylating site ($K_m = 0.2$ μM) is saturated at micromolar ATP, and it is the high rate which agrees with the rate of cation transport.

A possible mechanism for the role of the low-affinity binding site is the formation of an EKMgATP complex of the enzyme or phosphoenzyme in either of its conformations, which would shift the $E_2K \rightleftharpoons E_1K$ equilibrium to the right [24]. Low-affinity binding to the enzyme as well as the phosphoenzyme has been shown in this paper. The $E_2K \rightleftharpoons E_1K$ transition appears to play a role in K^+ transport, as reflected in the neutral K^+/K^+ exchange mode displayed by red cells (K_m ATP = 0.1 mM [25]). This K^+/K^+ exchange mode has also been observed with pig kidney $(Na^+ + K^+)$-ATPase reconstituted into phospholipid vesicles [24]. Here the K_m ATP increases from 4 to 300 μM, with increasing P_i and Rb^+ concentration, i.e., phosphorylation and Rb^+ binding increase the K_m ATP.

In the absence of phosphorylation, the $E_2K \rightarrow E_1K$ transition can be driven by ATP in the absence of added Mg^{2+} [26–28] and thus does not require Mg^{2+}-induced nucleotide binding per se. However, under phosphorylating conditions the situation may be different. In addition, high $[Mg^{2+}]$ and [ATP] may inhibit the backward reaction [29], thereby shifting the equilibrium to the right. The $E_2K \rightarrow E_1K$ transition is considered to be rate-limiting in the overall ATPase reaction at high ATP concentrations [26]. The overall ATPase reaction is competitively inhibited by Ado*PP*[NH]*P*. The K_i value for Ado*PP*[NH]*P* in the ATPase reaction agrees with its K_d value for binding at the low-affinity site over a wide temperature range. All this indicates that Ado*PP*[NH]*P* and ATP compete for the same low-affinity site, and that this Mg^{2+}-induced site is functional in the ATPase reaction.

At first sight, one would then also expect agreement between the low-affinity K_m value for ATP and the low-affinity K_d value for Ado*PP*[NH]*P*, as earlier suggested by Robinson [7]. Actually, we find a great discrepancy between these two parameters, when measured over a wide temperature range. This discrepancy is probably caused by the contribution to K_m of partial reactions following the binding. Karlish and Yates [26] have derived the following relation between the K_m and the K_d at the low-affinity sites: $K_m = K_d/(1 + k \cdot \sum_{n=1}^{3} k_n^{-1})$, where k is the rate constant at saturating ATP for the $E_2K \rightarrow E_1K$ transition and k_n the rate constant for any of the subsequent reaction steps (phosphorylation, $E_1P \rightarrow E_2P$ transition and K^+-stimulated dephosphorylation, all in the forward direction). This formula not only demonstrates that K_m must be smaller than K_d, but also that the higher Σk_n^{-1} is relative to k, the lower the K_m is relative to the K_d. This probably explains our observations in Fig. 5 when going from high to low temperature. However, it does not invalidate our conclusion about the order of binding affinity, since Karlish and Yates have calculated a K_d of 0.45 mM for ATP at 20°C, while we determine a

K_d of 0.25 mM for Ado*PP*[NH]*P* at 24°C. Thus, the affinity order Ado*PP*[NH]*P* > ATP is upheld.

A functional role of the Mg^{2+}-induced low-affinity nucleotide binding sites is further indicated by the equal affinity order for the adenine nucleotides for steady-state ATPase activity and for binding in the presence of ouabain: Ado*PP*[NH]*P* > ATP > ADP > AMP. The deviating order for GTP, CTP and ITP may be due to differences in ouabain-sensitivity and K^+-sensitivity of their enzyme-nucleotide complexes.

The relation of low-affinity nucleotide binding to the neutral K^+/K^+ exchange transport mode and the $E_2K \rightleftharpoons E_1K$ transition, mentioned above, encounters a difficulty when we consider the nucleotide specificities. For the K^+/K^+ exchange the efficacy of ATP is larger than that of Ado*PP*[NH]*P* [30], while the reverse is true for low-affinity binding. ADP and GTP are inactive in the K^+/K^+ exchange [25], but are active in low-affinity binding. However, it should be kept in mind that the $E_2K \rightarrow E_1K$ transition and thus the K^+/K^+ exchange is not only dependent on low-affinity nucleotide binding but also on the subsequent conformational change of E_2K to E_1K. The latter may very well have a different nucleotide specificity. Another potential difficulty is the fact that the K^+/K^+ exchange is ouabain-sensitive, while we show in this paper that the low-affinity binding capacity is insensitive to ouabain. However, ouabain freezes the enzyme in the E_2 conformation by its stabilizing effect on the phosphoenzyme formed by inorganic phosphate, thus inhibiting the K^+/K^+ exchange even though low-affinity binding takes place.

In conclusion, the Mg^{2+}-induced low-affinity nucleotide binding site is located on the α-subunit of $(Na^+ + K^+)$-ATPase, outside the phosphorylation centre. Its binding capacity is heat-labile and is reduced by *N*-ethylmaleimide treatment but not by ouabain. Its functional role is suggested by the similar adenine nucleotide specificity and the equality of the K_d and K_i values for Ado*PP*[NH]*P* in binding and ATP-hydrolysis. This functional role may consist of an acceleration of the $E_2K \rightarrow E_1K$ transition.

References

1 Schuurmans Stekhoven, F.M.A.H., Swarts, H.G.P., De Pont, J.J.H.H.M. and Bonting, S.L. (1981) Biochim. Biophys. Acta 649, 533–540

2 Schoot, B.M., Schoots, A.F.M., De Pont, J.J.H.H.M., Schuurmans Stekhoven, F.M.A.H. and Bonting, S.L. (1977) Biochim. Biophys. Acta 483, 181–192

3 Jørgensen, P.L. (1974) Biochim. Biophys. Acta 356, 36–52

4 Schuurmans Stekhoven, F.M.A.H., Swarts,. H.G.P., De Pont, J.J.H.H.M. and Bonting, S.L. (1980) Biochim. Biophys. Acta 597, 100–111

5 Nørby, J.G. and Jensen, J. (1974) Ann. N.Y. Acad. Sci. 242, 158–167

6 Davies, O.L. and Pearson, E.S. (1934) J. R. Stat. Soc. Suppl. 1, 76–93

7 Robinson, J.D. (1976) Biochim. Biophys. Acta 429, 1006–1019

8 Yount, R.G., Babcock, D., Ballantyne, W. and Ojala, D. (1971) Biochemistry 10, 2484–2489

9 Sen, A.K., Tobin, T. and Post, R.L. (1969) J. Biol. Chem. 244, 6597–6604

10 Hansen, O., Jensen, J. and Nørby, J.G. (1971) Nature New Biol. 234, 122–124

11 Schoner, W., Beusch, R. and Kramer, R. (1968) Eur. J. Biochem. 7, 102–110

12 Post, R.L., Kume, S., Tobin, T., Orcutt, B. and Sen, A.K. (1969) J. Gen. Physiol. 54, 306s–326s

13 Bonting, S.L., Schuurmans Stekhoven, F.M.A.H., Swarts, H.G.P. and De Pont, J.J.H.H.M. (1979) in Na,K ATPase, Structure and Kinetics (Skou, J.C. and Nørby, J.G., eds.), pp. 317–330, Academic Press, New York

14 Peters, W.H.M., Fleuren-Jakobs, A.M.M., De Pont, J.J.H.H.M. and Bonting, S.L. (1981) Biochim. Biophys. Acta 649, 541–549

15 Moczydlowski, E.G. and Fortes, P.A.G. (1981) J. Biol. Chem. 256, 2346–2356

16 Schoot, B.M., De Pont, J.J.H.H.M. and Bonting, S.L. (1978) Biochim. Biophys. Acta 522, 602–613

17 Schoot, B.M., Van Emst-De Vries, S.E., Van Haard, P.M.M., De Pont, J.J.H.H.M. and Bonting, S.L. (1980) Biochim. Biophys. Acta 602, 144–154

18 Rempeters, G. and Schoner, W. (1981) Eur. J. Biochem. 121, 131–137

19 Schuurmans Stekhoven, F.M.A.H., Van Heeswijk, M.P.E., De Pont, J.J.H.H.M. and Bonting, S.L. (1976) Biochim. Biophys. Acta 422, 210–224

20 Hall, C. and Ruoho, A. (1980) Proc. Natl. Acad. Sci. U.S.A. 77, 4529–4533

21 Sachs, J.R. (1981) J. Physiol. 316, 263–277

22 Askari, A. and Huang, W. (1982) Biochem. Biophys. Res. Commun. 104, 1447–1453

23 Patzelt-Wenczler, R. and Schoner, W. (1981) Eur. J. Biochem. 114, 79–87

24 Karlish, S.J.D., Lieb, W.R. and Stein, W.D. (1982) J. Physiol. 328, 333–350

25 Simons, T.J.B. (1974) J. Physiol. 237, 123–155

26 Karlish, S.J.D. and Yates, D.W. (1978) Biochim. Biophys. Acta 527, 115–130

27 Beaugé, L.A. and Glynn, I.M. (1979) Nature 280, 510–512

28 Beaugé, L.A. and Glynn, I.M. (1980) J. Physiol. 299, 367–383

29 Glynn, I.M. and Richards, D.E. (1982) J. Physiol. 330, 17–43

30 Simons, T.J.B. (1975) J. Physiol. 244, 731–739